DEVELOPMENT OF TRACTION CONTROL SYSTEM FOR ELECTRIC UNMANNED GROUND VEHICLE

Joonas Paales, Gregor Randla, Yevhen Ihnatiev, Tormi Lillerand, Juri Olt
Estonian University of Life Sciences, Estonia
joonas.paales@emu.ee, gregor.randla@emu.ee, yevhen.ihnatiev@emu.ee,
tormi.lillerand@emu.ee, jyri.olt@emu.ee

Abstract. This study presents the development of a traction control system (TCS) for a four-wheel electric unmanned ground vehicle (UGV) with four in-wheel motors and a passive articulated joint. Because the vehicle has no dedicated steering mechanism, turning is achieved by differential wheel-speed control, while the articulation angle develops passively from wheel-ground interaction. The proposed TCS combines kinematic wheel-speed allocation, quasi-static load-based traction redistribution, speed-error feedback and slip reduction in a low-cost embedded architecture based on Raspberry Pi Zero 2 W, dual IMUs, CAN telemetry and a four-channel digital-to-analog converter. For the investigated vehicle geometry, the maximum articulation angle of 30 deg corresponds to a minimum turning radius of 1.87 m, with outer and inner wheel path radii of approximately 2.30 and 1.40 m, respectively. The slip controller maintains full command up to a slip ratio of 0.15 (15%) and then progressively reduces wheel command as slip increases. Steering tests confirmed stable left-right wheel-speed differentiation under a maximum wheel-speed limit of 1.4 m s^{-1}, while the acceleration channel increased command when measured wheel speed fell below the reference. The developed TCS provides a practical basis for further field validation of passively articulated electric UGVs on soft and uneven terrain.

Keywords: traction control, unmanned ground vehicle, differential steering, articulated vehicle.

Introduction

Unmanned ground vehicles are increasingly used in agricultural operations, where soft soil, uneven terrain and tight manoeuvring place strong demands on traction management [1-5]. Recent studies on agricultural and off-road UGVs have addressed coordinated torque distribution, differential steering, path tracking and stability control for six-wheel independent-drive platforms, skid-steer robots and articulated vehicles [3-8]. Parallel work has improved trajectory tracking for agricultural robots and demonstrated the importance of accurate attitude and velocity estimation from IMU and wheel-sensor data [9-15]. In addition, wheel-load estimation and terrain interaction analysis have been used to improve traction allocation and mobility on soft ground and slopes [16-18]. Thus, the current state of the art increasingly combines distributed electric drive control with vehicle-state estimation and traction-oriented control logic.

Despite this progress, limited attention has been paid to compact four-wheel electric UGVs with passive articulation and no dedicated steering actuator. In such vehicles, steering must be produced electronically by left-right wheel-speed differentiation, while the articulation angle is not directly controlled and develops from wheel-ground interaction. As a result, reference wheel speeds, section-wise load redistribution and slip limitation must be solved simultaneously rather than as separate control problems.

The aim of this study is to develop and evaluate a traction control system (TCS) that converts speed and curvature inputs into wheel-specific commands for differential steering, speed tracking and slip reduction. The developed implementation combines a simplified kinematic steering model with section-wise attitude sensing in embedded architecture suitable for a compact electric UGV.

Materials and methods

UGV is electric, equipped with four motors, passively articulated and lacks an active steering mechanism, so steering must be accomplished by differential steering. Torque is provided by four BLDC in-wheel motors with individual ND72300 motor controllers. The system is supplied by a 48 V battery pack. A 12 V power supply powers a USB hub and a 5 V power supply powers a Raspberry Pi Zero 2 W, which serves as the TCS controller, and a Raspberry Pi 5, which serves as the central control unit. The USB hub allows data transfer between the TCS controller and the front and rear IMUs, which are OpenLog Artemis IMUs. The TCS controller is connected to a four-channel MCP4728 digital-to-analog converter, which provides throttle command signals to the motor controllers. Fig. 1 presents the electrical schematic of the UGV.

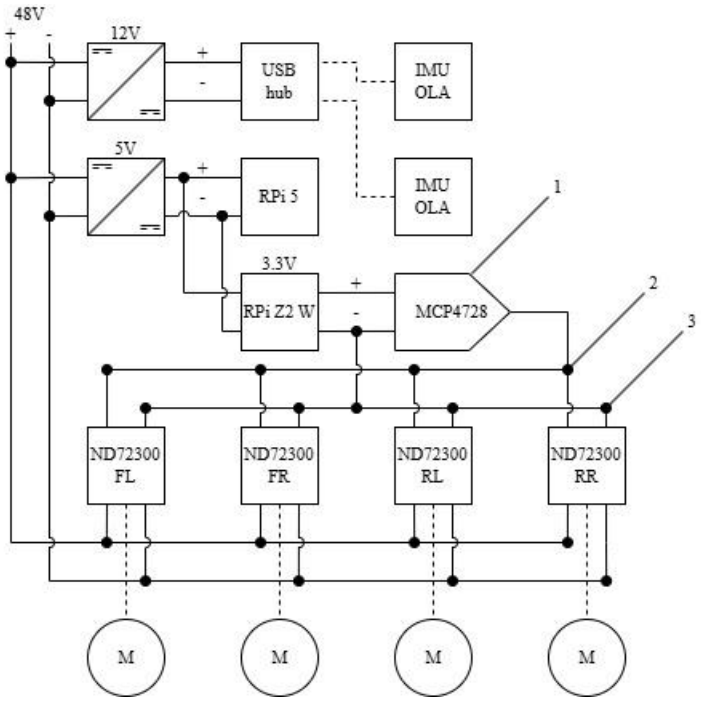

Fig. 1. **UGV electrical schematic:** 1 – four-channel DAC; 2 – throttle signal line; 3 – throttle ground line

The motor controllers enable CAN bus communication. This allows the TCS controller to read telemetry such as wheel speed, torque, voltage and phase current, and to transmit messages for motor direction and speed modes. IMUs are equipped with accelerometers and gyroscopes. Their data enable acquisition of section attitudes needed for articulated-vehicle state estimation, while wheel speed and controller telemetry provide a practical low-cost basis for feedback control and logging [12-15; 24]. The TCS controller logs telemetry data, inputs and IMU data into a SQLite database for further analysis. Fig. 2 depicts the TCS logic diagram.

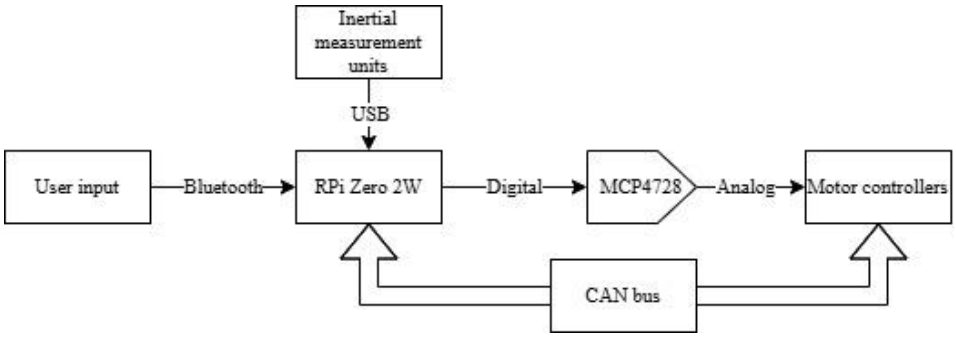

Fig. 2. **TCS logic diagram**

The vehicle consists of a front and a rear section, each carrying one left and one right driven wheel. Because neither steerable wheel knuckles nor an actuated articulation joint are available, a turn is generated by increasing wheel speeds on one side and reducing them on the other. The articulation angle is therefore a passive state variable resulting from wheel-ground interaction rather than a directly actuated control input. The control strategy contains three stages: first, reference speed and steering curvature are converted into left and right wheel-speed references using the vehicle geometry; second, front and rear IMU pitch and roll data are used in a quasi-static model to estimate wheel-load bias factors; third, measured wheel speeds are used to form the speed-feedback and slip-reduction terms. The final command for each wheel is obtained as the product of the load-share command, the acceleration command and the slip-reduction command, after which a rate limiter smooths the output before transmission through DAC.

The traction distribution model assumes that the centres of mass of both sections are at equal height and equally spaced from the articulation joint. This quasi-static representation is appropriate for low-speed maneuvering and allows the controller to bias traction according to section pitch and roll, which are key indicators of load transfer and terrain interaction [12; 16-18]. Fig. 3 defines the principal dimensions and mass locations used in the simplified vehicle model, and Table 1 lists the main characteristics of the UGV.

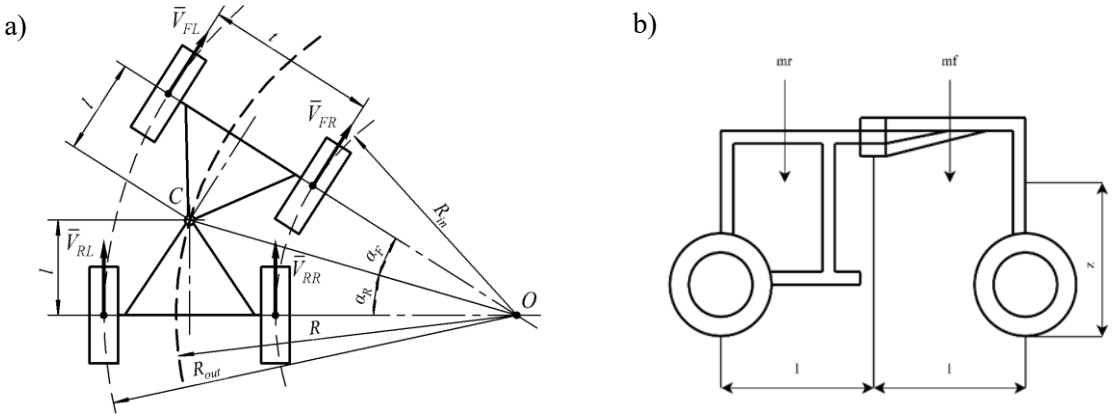

Fig. 3. **UGV kinematic scheme of turning a) and side view b) with principal dimensions**

Figure 3a shows the kinematic scheme of turning an articulated UGV, each wheel of which is given a corresponding speed V_{FL}, V_{FR}, V_{RL} and V_{RR} depending on the turning radius R and slippage. The kinematic center of the UGV, point C, makes a turn around the turning center, point O. The angles of rotation of the half-frames are denoted as α_F and α_R, and the radii of movement of the inner and outer wheels are R_{in} and R_{out}, respectively.

Table 1

UGV characteristics

Parameter	Symbol	Value
Centre of mass height	z	0.48 m
Mass of front section	m_f	160 kg
Mass of rear section	m_r	190 kg
Section length	l	0.50 m
Track width	t	0.87 m
Wheel radius	r	0.18 m

The inputs for TCS are reference speed and steering curvature. This allows the UGV to follow a stable path at a desired speed. Because the vehicle sections are symmetrical in width and length, the turning geometry can be represented by inner and outer wheel paths, which is consistent with articulated and differential-steered vehicle kinematics described in previous studies [6-8; 22; 23].

The maximum articulation angle of the UGV is 30 deg. This sets the minimum turning radius at 1.87 m, with approximately 2.30 m for the outer wheels and 1.40 m for the inner wheels. As the input controls the vehicle speed and curvature, the corresponding inner and outer wheel reference speeds are calculated [6; 8; 22; 23].

Wheel load is estimated using a quasi-static model that accounts for the section masses and the measured pitch and roll angles. As the section pitch increases, longitudinal load shifts between the front and rear sections, while the section roll redistributes the load between the left and right wheels. Similar use of vehicle dynamics and wheel-ground interaction information has been reported for terrain assessment and traction analysis in off-road agricultural robots [16-18].

Dividing the wheel load by the total vehicle mass gives a proportional estimate of the traction available for each wheel. Normalizing these values by the average wheel load yields a biasing factor that preserves the overall command level while redistributing it across the wheels. The final throttle command for each wheel is the product of the load-share command, the acceleration command and the slip-reduction command. Slip reduction is only activated when the slip ratio exceeds the configured target, which is consistent with slip-optimisation approaches used in traction-energy balancing and

distributed-drive controllers [3; 19-21]. The acceleration command takes the normalized speed request and adds the normalized speed error multiplied by the configured feedback gain. A rate limiter is applied to the final wheel commands to prevent abrupt changes that could induce additional slip or oscillation in low-traction conditions [3; 19-21].

Results and discussion

Fig. 4 shows the law by which the developed system handles the slip limitation. The controller actively counteracts slip up to 15%, and then gradually reduces the activity as the slip increases. When slip becomes excessive, the counteraction is reduced, and the torque is reduced also. This confirms that the controller limits slip without penalizing normal rolling [3; 19; 20]. Fig. 5 shows successful differential steering. For testing, maximum wheel speed was set a 1.4 $m \cdot s^{-1}$. This also limits the maximum reference speed. If the reference speed for left or right wheels would exceed the maximum, a new reference speed is calculated which sets the maximum speed of the outer wheels to 1.4 $m \cdot s^{-1}$. The controller splits the reference speed into left and right wheel commands so that one side accelerates while the other is reduced. This wheel-speed asymmetry enables turning without a mechanical steering linkage or actively actuated articulation, confirming that the kinematic steering model produces feasible wheel-speeds for articulated and differential-drive agricultural vehicles [6-8; 22; 23].

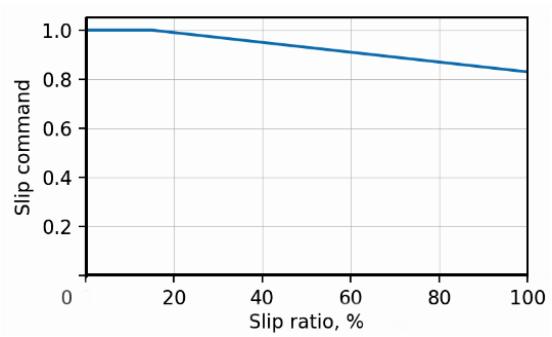

Fig. 4. **Wheel slip control command value**

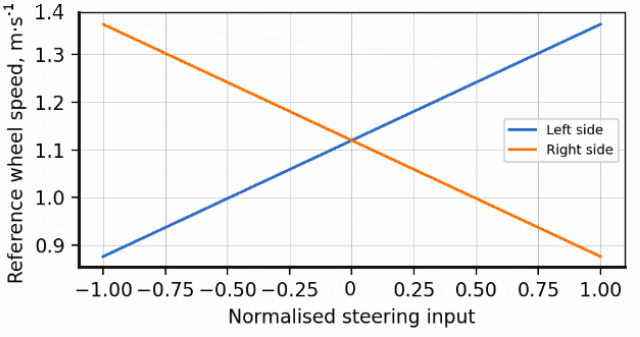

Fig. 5. **UGV left and right wheel speeds based on steering input**

Fig. 6 compares the acceleration gain command with the throttle input. The two curves follow the same overall trend, but the acceleration gain is adjusted by the speed-feedback term. As a result, command generation is not open-loop: it increases when the actual wheel speed falls below the reference and decreases when tracking is already adequate [20; 21].

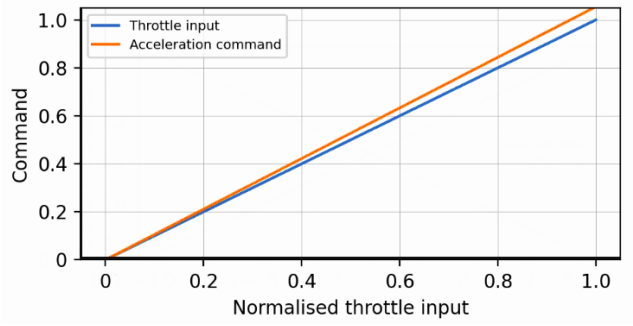

Fig. 6. **Input throttle and acceleration command**

Taken together, Figs. 4-6 show that the developed TCS performs its three main functions: slip limitation, differential steering and speed-error compensation. The present results are based on logged internal signals, so they validate the implemented control logic rather than full vehicle performance under all terrain conditions.

Field tests are still required to tune the acceleration feedback and slip-reduction coefficients and to quantify the benefit of load-aware traction distribution during demanding maneuvers, such as climbing a 15 deg ramp into a mobile charging station. Additional tests should compare the proposed controller with a baseline controller without load redistribution.

Conclusions

1. A traction control system was developed for a passively articulated electric UGV with four in-wheel motors using CAN telemetry, two IMUs, a Raspberry Pi Zero 2 W and a four-channel DAC interface.
2. The novelty of the research is the combination of a simplified kinematic steering model for a four-wheel UGV without steerable wheels or an actuated articulation joint, section-wise attitude sensing of the front and rear bodies, and load-aware traction redistribution integrated with slip limitation. Tests of the studied UGV showed that a 30 deg articulation limitation corresponds to a minimum turning radius of 1.87 m, with approximately 2.30 m and 1.40 m outer and inner radii of the wheel trajectory, respectively.
3. Studies have shown that the developed system maintains full control up to 15% slippage, and steering tests have confirmed the necessary differentiation of the speed of the left and right wheels and the limitation of the maximum wheel rotation speed of 1.4 $m \cdot s^{-1}$.
4. The developed system validates the intended control logic and provides a basis for further field experiments. Future work should quantify the vehicle performance on slopes and uneven terrain, including comparison with a baseline controller without load redistribution and tests of demanding manoeuvres.

Author contributions

Conceptualization, J.P. and Y.I.; methodology, T.L. and Y.I.; software, J.P and G.R..; validation, J.P. and T.L; formal analysis, J.P and G.R.; investigation, J.P..; data curation, J.P. and T.L.; writing original draft preparation, J.P.; writing review and editing, T.L. and Y.I.; visualization, J.P. and Y.I.; project administration, J.O. and T.L.; funding acquisition, J.O. All authors have read and agreed to the published version of the manuscript.

References

[1] Liu L., Yang F., Liu X., et al. A review of the current status and common key technologies for agricultural field robots. Computers and Electronics in Agriculture, vol. 227, 2024, article 109630. DOI: 10.1016/j.compag.2024.109630.

[2] Soots K., Lillerand T., Jogi E., Virro I., Olt J. Feasibility analysis of cultivated berry field layout for automated cultivation. Engineering for Rural Development, vol. 20, 2021, pp. 1003-1008. DOI: 10.22616/ERDev.2021.20.TF222.

[3] Xu X., Chen G., Gao X., et al. Stability and energy-saving coordinated control strategy of six-wheel independent drive unmanned ground vehicle. ISA Transactions, vol. 143, 2023, pp. 692-706. DOI: 10.1016/j.isatra.2023.10.001.

[4] Jiang Y., Meng H., Chen G., et al. Differential-steering based path tracking control and energy-saving torque distribution strategy of 6WID unmanned ground vehicle. Energy, vol. 254, 2022, article 124209. DOI: 10.1016/j.energy.2022.124209.

[5] Chen G., Gao X., Zhao Y., et al. Attitude stability control for 6WID unmanned ground vehicle during steering: a collaborative controller considering minimizing tire slip energy loss. Energy, vol. 302, 2024, article 131918. DOI: 10.1016/j.energy.2024.131918.

[6] Wang Y., Liu X., Ren Z., et al. Synchronized path planning and tracking for front and rear axles in articulated wheel loaders. Automation in Construction, vol. 165, 2024, article 105538. DOI: 10.1016/j.autcon.2024.105538.

[7] Ren X., Liu H., Qin Y., et al. Trajectory optimization and stability control for a novel unmanned intelligent wheel-legged vehicles on unstructured terrains. Robotics and Autonomous Systems, vol. 182, 2024, article 104818. DOI: 10.1016/j.robot.2024.104818.

[8] Antoshchenkov R., Halych I., Nikiforov A., Cherevatenko H., Sheptun S. Study of inter-wheel differential influence on dynamics of traction and transport machine. Engineering for Rural Development, vol. 24, 2025, pp. 234-241. DOI: 10.22616/ERDev.2025.24.TF046.

[9] Nadykto V., Arak M., Olt J. Theoretical research into the frictional slipping of wheel-type undercarriage taking into account the limitation of their impact on the soil. Agronomy Research, vol. 13(1), 2015, pp. 148–157.

[10] Zhang S., Wei X., Liu C., et al. Adaptive path tracking and control system for unmanned crawler harvesters in paddy fields. Computers and Electronics in Agriculture, vol. 230, 2025, article 109878. DOI: 10.1016/j.compag.2024.109878.
[11] Samaniego Sanchez J.A., Lopez-Gonzalez E., Magid E., Martinez-Garcia E.A. Double spiraliform path planning and tracking for agricultural mobile robotics: A modeling and simulation study. Computers and Electronics in Agriculture, vol. 237, 2025, article 110715. DOI: 10.1016/j.compag.2025.110715.
[12] Xu X., Lu S., Jiang Y., et al. Driving strategy of unmanned ground vehicle under split-docking road conditions based on improved EKF and PID-modified SMC. Advanced Engineering Informatics, vol. 62, 2024, article 102830. DOI: 10.1016/j.aei.2024.102830.
[13] Wei X., Fan S., Zhang Y., et al. A robust adaptive error state Kalman filter for MEMS IMU attitude estimation under dynamic acceleration. Measurement, vol. 242, 2025, article 116097. DOI: 10.1016/j.measurement.2024.116097.
[14] Le N.T., Truong C.T., Nguyen H.H., et al. Yaw angle determination of a mobile robot operating on an inclined plane using accelerometer and gyroscope. Measurement, vol. 247, 2025, article 116806. DOI: 10.1016/j.measurement.2025.116806.
[15] Seo D., Kang J. Dynamic-Model-free vehicle velocity estimation using extended Kalman filter with IMU, steering Angle, and wheel speed sensors. Measurement, vol. 242, 2025, article 115810. DOI: 10.1016/j.measurement.2024.115810.
[16] Mu X., Li Z., Ji Y., et al. Influence of track ground pressure distribution uniformity on traction under slope. Biosystems Engineering, vol. 257, 2025, article 104252. DOI: 10.1016/j.biosystemseng.2025.104252.
[17] Adamchuk V., Bulgakov V., Nadykto V., Ihnatiev Y., Olt J. Theoretical research into the power and energy performance of agricultural tractors. Agronomy Research, vol. 14(5), 2016, pp. 1511–1518.
[18] Zheng X., Cai R., Xiao S., et al. Primary-auxiliary model scheduling based estimation of the vertical wheel force in a full vehicle system. Mechanical Systems and Signal Processing, vol. 187, 2023, article 109946. DOI: 10.1016/j.ymssp.2022.109946.
[19] Liang Y., Zhao W., Wu J., et al. Energy-efficient driving for distributed electric vehicles considering wheel loss energy: a distributed strategy based on multi-agent architecture. Applied Energy, vol. 384, 2025, article 125462. DOI: 10.1016/j.apenergy.2025.125462.
[20] Xu T., Zhao Y., Deng H., et al. Integrated optimal control of distributed in-wheel motor drive electric vehicle in consideration of the stability and economy. Energy, vol. 282, 2023, article 128990. DOI: 10.1016/j.energy.2023.128990.
[21] Li Z., Wang P., Liu H., Hu Y. Integrated predictive motion control for electric vehicles: A fast solution for safety and control-constrained optimization. Advanced Engineering Informatics, vol. 68, 2025, article 103597. DOI: 10.1016/j.aei.2025.103597.
[22] Hernandez Sanchez A., Poznyak A., Chairez I. Extremum seeking control for the trajectory tracking of a skid steering vehicle via averaged sub-gradient integral sliding-mode theory. Robotics and Autonomous Systems, vol. 174, 2024, article 104609. DOI: 10.1016/j.robot.2023.104609.
[23] Bulgakov V., Ivanovs S., Adamchuk V., Antoshchenkov R. Investigations of the Dynamics of a Four-Element Machine-and-Tractor Aggregate. Acta Technologica Agriculturae, vol. 22(4), 2019, pp. 146–151. DOI: 10.2478/ata-2019-0026.
[24] Jensen K.M., Santos I.F., Corstens H.J.P. Towards mass estimation of passenger cars based on longitudinal dynamics without considering vehicle CAN-bus data. Mechanical Systems and Signal Processing, vol. 223, 2025, article 111907. DOI: 10.1016/j.ymssp.2024.111907.
[25] Kubas J., Ballay M. Development of charging infrastructure with regard to differences of regions in environment of Slovakia. Engineering for Rural Development, vol. 22, 2023, pp. 439-444. DOI: 10.22616/ERDev.2023.22.TF093.